Lab on a Chip

Placental microphysiological systems: New advances on promising platforms that mimic the microenvironment of the human placenta

Journal:	*Lab on a Chip*
Manuscript ID	LC-CRV-06-2024-000500.R1
Article Type:	Critical Review
Date Submitted by the Author:	17-Sep-2024
Complete List of Authors:	Gonçalves, Inês; Tokyo Medical and Dental University Afzal, Muhammad; Tokyo Medical and Dental University Kennedy, Nithil; Tokyo Medical and Dental University Moita, Ana; Universidade de Lisboa Lima, Rui; University of Minho, Mechanical Engineering Department; University of Porto, CEFT - Centro de Estudos de Fenómenos de Transporte, Faculdade de Engenharia, Universidade do Porto Ostrovidov, Serge; Tokyo Medical and Dental University Hori, Takeshi; Tokyo Medical and Dental University, Division of Diagnostic & Therapeutic Systems Engineering Nashimoto, Yuji; Tokyo Medical and Dental University Institute of Biomaterials and Bioengineering, ; Tohoku University, Frontier research institute for interdisciplinary sciences Kaji, Hirokazu; Tokyo Medical and Dental University, Institute of Biomaterials and Bioengineering

ARTICLE

Received 00th January 20xx,
Accepted 00th January 20xx

DOI: 10.1039/x0xx00000x

Placental microphysiological systems: New advances on promising platforms that mimic the microenvironment of the human placenta

Inês M. Gonçalves,[abc] Muhammad Afzal,[c] Nithil Kennedy,[cd] Ana Moita,[be] Rui Lima,[afg] Serge Ostrovidov,[c] Takeshi Hori,[c] Yuji Nashimoto,[c] and Hirokazu Kaji, [c *]

[a] METRICS, University of Minho, Guimarães, Portugal

[b] IN+, Instituto Superior Técnico, Universidade de Lisboa, Lisboa, Portugal

[c] Department of Diagnostic and Therapeutic Systems Engineering, Institute of Biomaterials and Bioengineering (IBB), Tokyo Medical and Dental University (TMDU), 2-3-10 Kanda-Surugadai, Chiyoda-ku, Tokyo 101-0062, Japan.

[d] Faculty of Medicine, Imperial College London, London, United Kingdom

[e] Centro de Investigação Desenvolvimento e Inovação da Academia Militar, Academia Militar, Instituto Universitário Militar, Rua Gomes Freire, 1169-203, Lisboa, Portugal

[f] CEFT, Faculty of Engineering of the University of Porto, Porto, Portugal

[g] ALiCE, Faculty of Engineering, University of Porto, Porto, Portugal

*E-mail: kaji.bmc@tmd.ac.jp

One of the most complex human physiological processes to study is pregnancy. Standard animal models, as well as two-dimensional models lack the complexity and biological relevance required to accurately study such physiological process. Recent studies have focused on the development of three-dimensional models based on microfluidic systems, designated as placental microphysiological systems (PMPS). PMPS devices provide a model of placental barrier through culturing relevant cell types in specific arrangements and mediums to mimic the in vivo environment of the maternal-fetal circulation. Here, recent developments of PMPS models for embryo uterine implantation, preeclampsia evaluation, and toxicological screening are presented. Studies that use bioprinting techniques are also discussed. Lastly, recent developments in endometrium microphysiological systems are reviewed. All these presented models showed their superiority compared to standard models in recapitulating the biological environment seen in vivo. However, several limitations regarding the type of cells and materials used for these systems were also widely reported. Despite the need for further improvements, PMPS models contribute to a better understanding of the biological mechanisms surrounding pregnancy and respective pathologies.

Introduction

The placenta is a vital organ for the growth and formation of a fetus. Its primary function during the early stages of pregnancy is to safely attach to the lining of the uterus and establish contact with the fetus[1]. Later, the placenta develops into a series of cell layers originating from both the mother and the fetus and adopts the role of the intestines, liver, lungs, kidneys and endocrine glands.[1,2] Immediately following embryo implantation, cytotrophoblasts emerge and undergo fusion and differentiation to give rise to syncytiotrophoblasts. A representation of the placenta formation is presented in Figure 1. The chorion frondosum of fetal origin, and the decidua basalis of maternal origin develop into the fetal and maternal portions of the placenta, respectively. The placenta then develops during

[a.] Address here.
[b.] Address here.
[c.] Address here.
† Footnotes relating to the title and/or authors should appear here.
Supplementary Information available: [details of any supplementary information available should be included here]. See DOI: 10.1039/x0xx00000x

the remaining stages of pregnancy as the primary organ that supports the fetus' growth until birth, facilitating vital nutrient exchange between the maternal and fetal blood.[3] It is important to recognize that the placenta serves as more than just a semipermeable membrane through which substances can move back and forth between the mother and the fetus. In fact, transport across the placenta is influenced by several variables including growth and metabolic requirements of placental tissue. Placental transport is further dependent on blood flow through maternal and fetal placental compartment, concentration gradients of chemical substances and availability as well as localization of placental transporters[3]. The placenta can distinguish between demand signals from the fetus and supply signals from the mother, integrating these signals to control the placental exchange function[1,4,5]. Placental trophoblasts protect the fetus from the mother's immune system, preventing rejection upon exposure to maternal cells. Consequently, healthy development of the placenta is crucial for a pregnancy without complications. However, specific physiological processes within the human placenta are poorly understood and mechanisms behind placental pathophysiology and complications in pregnancy are yet to be elucidated.[2,3,6]

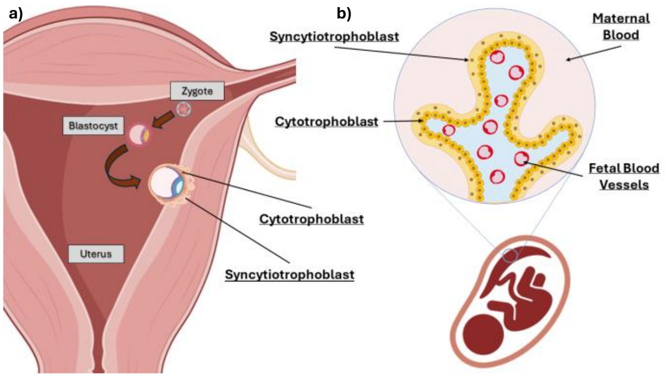

Figure 1. Illustration of a) human blastocyst implantation in the uterus and b) subsequent placenta formation.

Our knowledge about the placenta is primarily gathered from explants at term or from unsuccessful pregnancies. The scope for *in vivo* models is limited due to ethical implications. Additionally, viable explants are scarce and start to deteriorate shortly after being collected, which makes them unsuitable for experimentation since they cannot be sustained for extended study periods.[4]

Considering animal models, mice have been used to study the placenta due to the genetic consistency with humans and relative ease in manipulating their genome. However, there are substantial differences between mice and humans in terms of trophoblast cell types and placental structures.[2,4] Therefore, the principal methods of studying the human placenta have been through primary cultures, choriocarcinoma cell lines and immortalized cell lines. However, primary trophoblast cells have proved challenging to maintain in culture, and choriocarcinoma and immortalized cell lines are limited in reproducing the complex placental architecture and may have potentially several molecular pathways disrupted.[2] One essential step in improving further the studies on human placenta was the establishment of human trophoblasts stem cells (TSs). Okae et al.[7] were able to derive TS cells from blastocysts and early placentas by activating the Wingless/Integrated (Wnt) and epidermal growth factor (EGF) signaling pathways and by using inhibitors of transforming growth factor-beta (TGF-β), histone deacetylase (HDAC), and Rho-associated protein kinase (ROCK) in the culture medium.[2] A novel method for examining placenta metabolic activity in both simple and complex pregnancies is to use three-dimensional (3D) models, microphysiological systems (MPS) such as organoids or organs-on-chip, that preserve cellular interactions ex vivo[3]. The combination of several types of cells with 3D culture systems will provide a deeper understanding of the physiological and chemical mechanisms underpinning placenta formation and function[2].

The Placental MPS (PMPS) model, combines microfluidics with various human placental cells in 3D structures to produce a novel therapeutic tool that displays promising organotypic aspects of the placenta.[8] In this review, we present several PMPS models and respective cell types that have been used in recent studies. Other placenta models are also reviewed, as well as endometrium-on-a-chip models. The results obtained from such studies have contributed to a deeper understanding of the cellular mechanisms between maternal and fetal cells. They have also enabled insights into evaluating the effects of several chemicals and nanoparticles. However, a true representation of the placenta is still yet to be achieved and calls for further improvement to existing models.

Placental Microphysiological System Devices

The MPS are powerful tools in understanding the physiology of the human body. These advanced microfluidic devices facilitate embedding 3D culture cells in perfusion chambers to mimic the complex 3D microenvironments seen *in vivo* (Figure 2).[9,10] Microfluidic devices are usually prepared with the use of soft lithography techniques. However, due to the high fabrication costs and time taken for production, more recently other strategies such as bioprinting or laser cutting and Plexiglass are often used to fabricate the microfluidic devices[9,11–13]. Bioprinting is a layer-by-layer deposition technique allowing for rapid printing of various materials and complex 3D constructions with cells in a bioink[14–16]. Polydimethylsiloxane (PDMS) is frequently employed to make these devices, due to its unique properties such as biocompatibility, gas permeability, transparency, and flexibility[17,18]. However, PDMS presents a serious limitation as hydrophobic molecules can be adsorbed on its surface. As a result, other materials such as fluoroelastomer have been proposed as an alternatives to fabricate microfluidic devices[9,19,20].

To better understand the physiology surrounding pregnancy and the respective pathologies, recent studies have focused on the development of MPS that replicate the placental cellular structure. The most common models present two channels on top of each other, separated by a porous membrane which that are usually used for the study of substance transfer between the mother and the fetus. Other type of common devices has three channels that can be separated by microposts or open so surface tension forces could act. Those devices are more commonly used for the study of cellular mechanisms.

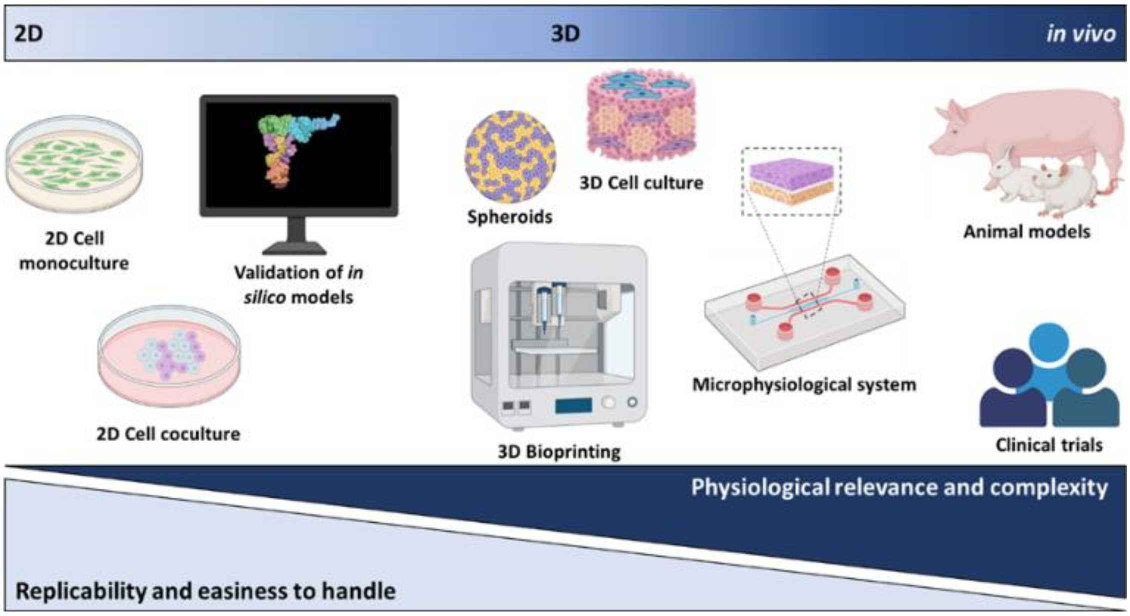

Figure 2. Schematic representation of different models used for the study of the human physiology regarding their replicability and physiological relevance.

Uterine Implantation Models

Govindasamy et al.[21] developed a PMPS model to assess the trophoblast invasion that occurs during the first interactions between the embryo and the maternal vasculature. The PMPS device has two PDMS channels embedded in a hydrogel. Mouse endothelial cells (bEnd5) were cultured in the channels and blastocysts were placed in proximity to the channels. The blastocysts were obtained from superovulated B6C3F1 female mice that mated with transgenic reporter or wild type males. In this model, it was possible to observe an implantation process similar to the one reported *in vivo*. The authors showed a number of adhesion molecules, vascular receptors and ligands that contributed to the mediation of the implantation. Especially, the platelet-derived growth factor (PDGF) was studied in depth since its signaling lead to the creation of heterologous connections. Furthermore, inhibition of this factor affected the first stage of pregnancy through the communication between the maternal blood vessels and the mouse embryo. However, it was noted that this PMPS platform was still not able of fully replicating the complexity of the environment seen *in vivo*. In another study, Miura et al.[22] presented a PMPS to investigate the effects of fluid shear stress (FSS) on the microvilli formation in human placental trophoblastic cells. The device consists of two PDMS channels forming a cross-section separated by a 10 µm thick vitrified collagen (VC) membrane. BeWo trophoblastic cells were cultured on the maternal side of the membrane. The authors compared the number of villi on cells in static conditions and on cells subjected to different ranges of culture medium flow rate. Under static conditions, the cells exhibited growth of few microvilli. On the other hand, when subjected to flow rate, the number of microvilli increased significantly. The length of the villi was also influenced by the flow rate. Additionally, the authors highlighted the importance of calcium ion influx for microvilli formation and on the importance of the calcium ion channel vanilloid family type-6 (TRPV6) in the process. Moreover, Park et al.[23] developed a microfluidic model to mimic the implantation events that occur during early pregnancy and reflect the invasion of the maternal uterus by specialized fetal extravillous trophoblasts (EVTs). The device was made of PDMS and consisted of three parallel channels with a gap between them. The middle channel was filled with a hydrogel of extra-cellular matrix (ECM) containing decidualized stromal cells (DSCs), normal human lung fibroblasts (NHLFs), human tracheal epithelial cells (hTECs), and/or uterine natural killer cells (uNKs). Primary EVT were cultured on one of the side channels while maternal endothelial cells were placed on the other side channel. The researchers reported a migration of EVTs toward the maternal compartment with the endothelial cells as observed *in vivo*. It was also noted that DSCs have a significant influence on the regulation of the EVT migration. Interestingly, this microfluidic model also enabled the evaluation of the effect of maternal immune cells on the EVT invasion. The uNKs were isolated and cultured with EVTs and uterine endothelial cells and a significant increase not only in the invasion depth and the invading cell number but also in the rate of the EVT migration was observed. In contrast, the EVT invasion was substantially reduced when uNKs and DSCs were used together as compared to the other two cases: EVTs+ECs and EVTs+ECs+uNKs. It was concluded that the uNKs play an important role in the invasion of EVTs and favor it. In addition, the remodeling of maternal spiral arteries by the fetal EVTs, a vital process that establishes proper exchange of materials between the mother and fetus, was also discussed. The EVTs continuously moved through the ECM compartment and reached the maternal vessel by breaching the vascular compartment. This invasive pattern of EVTs rapidly disrupted the vascular endothelium. The study showed the apoptotic behavior of maternal endothelial vasculature by the activation and upregulation of cell death in a caspase-dependent manner. In another study, Abbas et al.[24] fabricated a microfluidic device with three parallel channels to study the cell migration that occurs during the implantation phase of the pregnancy. The central channel was filled with EVTs in Matrigel® while the two peripheral channels contained A) medium with human recombinant granulocyte macrophage colony stimulating factor (hrGM-CSF) and B) medium without hrGM-CSF but with continuous perfusion. Consequently, a cytokine gradient was established within the device. The authors reported that EVT migration was undirected without the chemical gradient, whereas in the presence of the gradient, EVTs displayed increased motility with direction and reduced velocity. Since hrGM-CSF is secreted by activated decidual natural killer cells, we can infer these cells play an important role in EVT migration. Furthermore, an antibody to block the effect of hrGM-CSF was also used and resulted in reduced migration but did not stop the EVT migration completely. Consequently, the authors concluded that there must be other factors that influence the migration process. Moreover, Mosavati et al.[25] also fabricated a PMPS model composed of a co-culture of BeWo cells and HUVECs on the top and on the bottom of a porous polycarbonate membrane, respectively. The glucose transport across the barrier was evaluated both experimentally and numerically with a good agreement. Both models showed a higher diffusion rate when no cells were cultured on the device. The diffusion rate lowered when a monoculture was seeded on the device and was the lowest when the co-culture was established. The numerical model allowed the researchers to study the effects of flow rate and membrane porosity on glucose transport and the results showed that the diffusion of glucose increased with the increase of membrane porosity while decreased with the increase of flow rate.

Table 1. Placental MPS models and cell lines used in recent studies of the cellular mechanics of the earlier stages of pregnancy. The figures are reprinted with permission from Govindasamy et al. [21] Copyright (2021) Elsevier In; Miura et al. [22] Copyright (2015) The Authors (open access); Park et al. [23] Copyright (2022) The Authors (open access); Abbas et al. [24] Copyright (2017) The Authors (open access); and Mosavati et al. [25] Copyright (2020 by the authors (open access).

<table>
<tr><th>Placenta-on-Chip</th><th>General Description</th><th>Cell Lines</th><th>Ref.</th></tr>
<tr><td>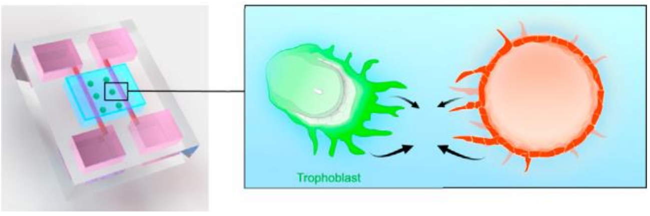
</td><td>Schematic illustration of the microfluidic chip based on methacrylated dextran, used to co-culture embryonic and endothelial cells, and of the interactions between trophoblasts and endothelial cells.</td><td>bEnd5, blastocysts</td><td>21</td></tr>
<tr><td>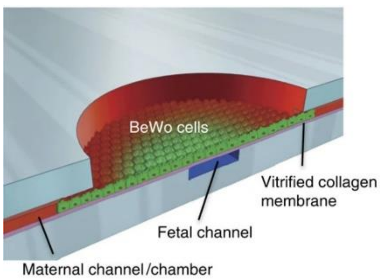
</td><td>Schematic illustration of the design of the PMPS. A vitrified collagen (VC) membrane is used to create PDMS microchannels (200 µm in height and 1 mm in width) that correspond to the flow rate of maternal and fetal blood. A chamber structure (ϕ = 4 mm) in the maternal microchannel resembles the large blood space of the intervillous region. By mixing red (for the mother) and blue (for the fetus), ink, we were able to see the maternal and fetal channels. The cell layer cultivated on the VC membrane served as the sole conduit for material transfer between the microchannels.

Scale bar: 1 cm</td><td>BeWo</td><td>22</td></tr>
</table>

Placenta-on-Chip	General Description	Cell Lines	Ref.
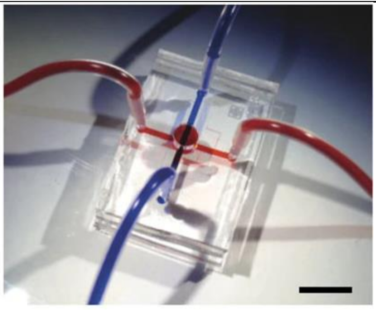			
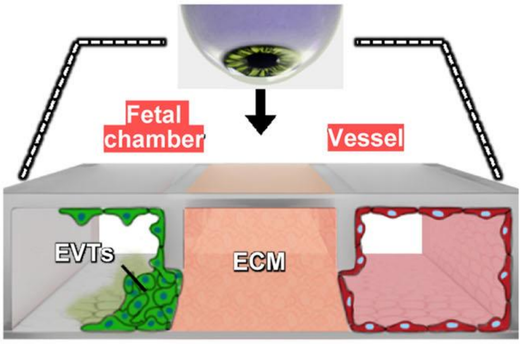	Schematic illustration of the three different channels of the PMPS: the maternal channel on the left with ECs, the middle channel filled with ECM and the fetal channel with EVTs. ECs: Endothelial cells ECM: Extracellular matrix EVTs: Extravillous trophoblasts	EVTs, DSCs	23
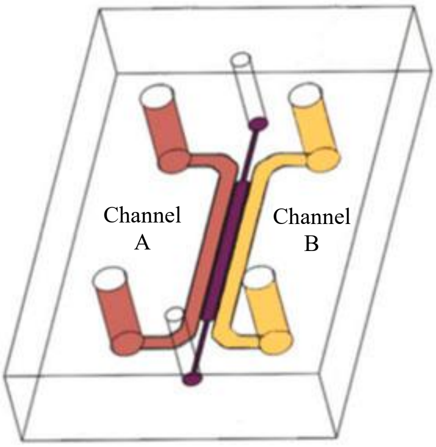	Schematic illustration of the PMPS used as a trophoblast invasion model. Stained EVTs were placed in Matrigel in the central channel. On the peripheral channels, a steady flow of medium, with (A) and without (B) hrGM-CSF was applied. EVTs: Extravillous trophoblasts hrGM-CSF: Human recombinant granulocyte-macrophage colony-stimulating factor	Trophoblasts	24
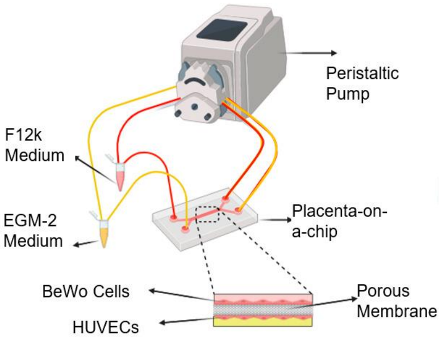	Schematic illustration of the experimental setup for the microfluidics-based model of the human placental barrier for glucose transfer analysis.	BeWo, HUVECs	25

Preeclampsia Models

Rabussier et al.[26,27] developed and implemented a model of placenta barrier to study preeclampsia. The device consists of three adjacent microchannels, two on either side for cell culture and one in the middle for the ECM scaffold. The ECM was prepared using a mixture of collagen-I and collagen-IV. BeWo cells were cultured on the maternal channel and, after 3 days, HUVECs were cultured on the fetal channel. Key characteristics such as thinning of the materno-fetal space, secretion of specific extracellular membrane components, transporter function, hormone secretion and polarization were reported by the authors, and recognized as physiologically relevant parameters by which to assess the device. The perfusion flow and the oxygen levels were modulated to induce preeclamptic characteristics which resulted in a reduction of microvilli, hormone secretion and barrier function. Furthermore, Ghorbanpour et al.[28] used a similar device where a first trimester trophoblast cell line (ACH-3P) and HUVECs were cultured on the peripheral channels and central channel, respectively. The central channel was also filled with an ECM matrix containing collagen type I. It has been observed that the inflammatory and vascular proteins galectin-3 (Gal-3) and FK506-binding protein like (FKBPL) had abnormal expressions in the case of preeclampsia. By exposing the cell cultures of the 3D model in the microfluidic device to the inflammatory cytokine tumor necrosis factor-α (TNF–α), a similar aberrant expression of Gal-3 and FKBPL was reproduced *in vitro*, which impaired the HUVECs to form a vascular network. Consequently, the proposed model could be used to further investigate the mechanisms involved in preeclampsia.

Table 2. Placental MPS models and cell lines used in recent studies of preeclampsia. The figures are reprinted with permission from Rabussier et al. [27] Copyright (2023) The Authors (open access); Ghorbanpour et al. [28] Copyright (2023) The Authors (open access).

Placenta-on-Chip	General Description	Cell Lines	Ref.
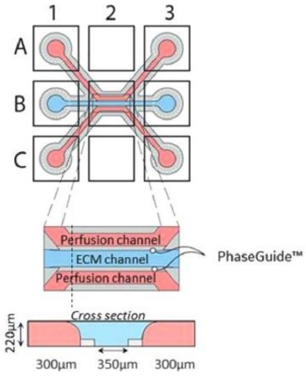	Schematic illustration of a single chip. Three neighboring channels are connected by top (A1), bottom (C1) inlets, and top (A3), bottom (C3) outlets wells. Small ridges (PhaseGuide™) that divide perfusion channels made it possible to pattern ECM gel in the central lane and culture cells in the perfusion channels without using a membrane. Through the observation window (B2), cultures were observed.	BeWo, HUVECs	26, 27
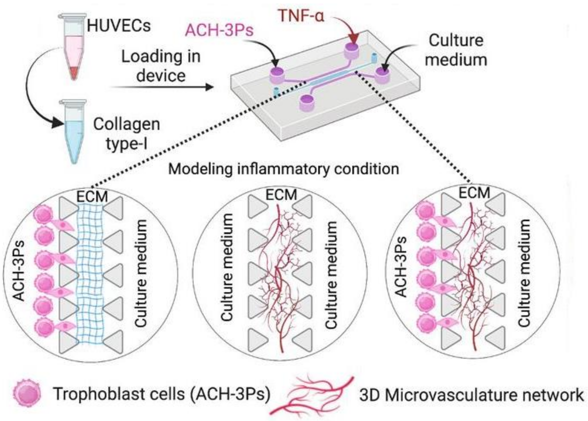	Placental samples and human plasma were examined for FKBPL and Gal-3 protein expression and circulation. A PMPS was created utilizing 3D microfluidic chips, with ACH-3Ps in the peripheral channel that migrated across and merged with the vasculature, HUVECs occupied the central channel containing ECM (Collagen type-I). FKBPL: FK506-binding protein-like Gal-3: galectin-3 ACH-3Ps: first trimester trophoblast cells HUVECs: Human umbilical vein endothelial cells ECM: Extracellular matrix	ACH-3Ps, HUVECs	28

Toxicology Screening Models

Some researchers developed PMPS models to evaluate the transport of specific substances between the mother and the fetus and their effects. Zhu et al.[29] recreated the fetal-maternal interface by manufacturing a PDMS PMPS device with two channels connected by a semipermeable membrane. Human trophoblast cells (BeWo cells) were cultured on one side of the membrane (maternal side) while HUVECs were on the other side (fetal side). Differentiated human macrophages (THP-1) were also cultured on the maternal side. Both cell cultures were under perfusion 10 µL/h and with time established a cellular cell barrier. The maternal channel was exposed to the bacteria *Escherichia coli* (*E. coli*) to simulate infection. On the maternal side, there was activation of macrophages and the secretion of inflammatory cytokines (IL-1a, IL-1b, IL-6, and IL-8) by the trophoblasts on the maternal side. Furthermore, when THP-1 were introduced onto the infected trophoblast layer, they became activated and attached to the cell layer. In addition, the secretion of inflammatory cytokines on the fetal side was also reported despite no bacteria have been found on that channel, which showed the strong transplacental communication. The authors concluded that this device could help understand fetal inflammatory response. Inclusion of more physiologically relevant cell types would further improve the applicability of this model.

Similarly, Blundell et al.[30] developed a PMPS device comprising of two PDMS microchannels bound together and separated by a semipermeable polycarbonate membrane with pores of 1 µm. Human placental vascular endothelial cells (HPVECs) were cultured on the bottom side of the membrane while BeWo cells were cultured on the upper side, to mimic the trophoblast–endothelial interface. Cells were cultured under dynamic flows and microvilli formation was observed on both cell types. The authors also reported the formation of syncytialized epithelium with the administration of forskolin and the expression of membrane-bound glucose transporters (GLUTs), with a rate of glucose transfer from the maternal to the fetal compartments similar to the one reported in *ex vivo* human placenta studies. Lee et al.[31] also developed a PMPS with two PDMS layers connected by a vitrified collagen type 1 membrane. Trophoblasts (JEG-3 cells) were cultured on the lower side of the membrane while green fluorescent protein (GFP)-expressing HUVECs were cultured on the top side, and with time a cellular barrier was established. Glucose transport through the cellular barrier was assessed. The results suggest that the transport over the barrier was controlled by mechanisms other than concentration gradient-induced passive diffusion due to the difference in glucose concentration in the upper and lower channels, and that the cells were a key factor in determining the glucose transfer, especially the trophoblast epithelium. Placental cells expressed glucose transporters which may explain how glucose was transferred in the device. Moreover, Pu et al.[32] used a commercially available PDMS device with a central chamber and two peripheral channels, where HUVEC and chorionic villi-derived first-trimester human placenta HTR8/SVneo trophoblast cells were cultured, respectively, to serve as a placenta model. The authors observed trophoblast invasion on the device through flow cytometry and transwell invasion assay. The device was then used to evaluate the invasiveness of two chemoattractants. Consequently, the platform showed the potential of the device for toxicological screening and to help the understanding of cell invasion mechanisms. In another study, Cao et al.[33] fabricated a PDMS PMPS device with two channels separated by a porous polyethylene terephthalate (PET) membrane (pore size 2 µm). On the maternal side TSs were seeded and their differentiation into syncytiotrophoblasts (STs) and cytotrophoblasts (CTs) was induced. On the fetal side HUVECs were seeded. The authors evaluated the effects of flow shear stress on the differentiation of TSs and reported that lower values of flow shear stress, such as approximately 0.005 dyn/cm^2, produced greater differentiation compared to higher flow shear stress values. The effects of the toxin mono-2-ethylhexyl phthalate (MEHP) were also evaluated using the PMPS model. No reports of direct toxicity to HUVECs were reported, while TS viability decreased with the increase of MEHP concentration. In addition, low doses of MEHP induced the differentiation of TS into EVTs which can be attributed to disturbances in trophoblast migration. Richardson et al.[34] designed and developed two platforms (FMI-OOC and PLA-OOC) that represent the human feto-maternal interfaces (FMis) and the placenta in terms of function and structure. They evaluated the effects and kinetics of the drugs pravastatin and rosuvastatin on these platforms. The FMi-OOC device was made of four concentric chambers connected by microchannels. From the center to the periphery, the chambers contained decidual cells, chorion trophoblast, amnion mesenchymal and epithelial cells. The PLA-OOC device was seeded with HUVECs, BeWo cells (cytotrophoblasts) and BeWo cells with forskolin (syncytiotrophoblasts). The drugs were added at a therapeutic concentration (200 ng.mL^{-1}) to the decidua (in FMI-OOC) and syncytiotrophoblasts chambers (in PLA-OOC) and their effects were evaluated in normal and oxidative stress conditions. The authors reported that, in around four hours, the tested medications penetrated the maternal-fetal cell layers of both devices. The production of cell- and time-specific statin metabolites from a variety of cell types without cytotoxicity was also registered. Statins successfully reduced oxidative stress-induced pro- inflammatory cytokines by enhancing anti-inflammatory cytokine response across the devices. The presented platforms proved to be an effective model to study the placenta, having the potential to mimic different stages of pregnancy according to the cell type cultured. However, the authors also highlighted that the devices lack dynamic flow, which should be improved in future works. Kim et al.[35] used the same FMi-OOC model with the same cells to evaluate the effect of the environmental toxin cadmium (Cd) on the FMi. The results showed that Cd only had a direct effect on the maternal cells. The effects on the fetal cells were minimal and only due to indirect effects. Consequently, these types of devices can contribute to the understanding of the mechanisms behind substance exposure. Furthermore, Blundell et al.[36] used a PDMS microfluidic chip with two overlayed channels separated by a porous polycarbonate membrane to study the drug transfer between the mother and the fetus during pregnancy. BeWo cells and human placental villous endothelial cells (HPVECs) were used for the maternal and fetal side, respectively. The transfer of the drug glyburide, commonly used for gestational diabetes, between the two channels was evaluated with and without cells. When no cells were present on the device, the concentration of the drug on the maternal channel remained the same. However, when the cell culture was established in the device, the concentration diminished over time. The researchers acknowledge the possible role of trophoblasts on the maternal side on the uptake of the drug. On the other hand, the concentration of the drug on the fetal side was constant and lower than the maternal side. Since no changes in drug concentration were reported when using a HPVEC monoculture, the researchers concluded that the BeWo cells are the main components in the mediation of drug transport in the PMPS model. In another study, Pemathilaka et al.[37] studied the transport of caffeine through the placenta using a PMPS device with two microchannels separated by a polyester track etched (PETE) membrane with a pore size of 0.4 µm. HUVECs and BeWo cells were cultured either side of the membrane. Caffeine was introduced on the maternal channel at a concentration of 0.25 mg mL^{-1} and the device was analyzed for 7.5 h. A concentration of 0.0033 mg.mL^{-1} was registered on the fetal side after five hours.

PMPS devices have also been used to study the transport and effect of nanoparticles (NPs) through the placenta. Thus, Gresing et al.[38]

used a commercial microfluidic device[39] as a PMPS model to study the transport of magnetic NPs. Different NPS were prepared, and the NPs were composed of an iron oxide core with a shell of SEON$^{LA\text{-}HSA}$, or sodium citrate (NaZ), citric acid (CA), or PEI-M. Firstly, the researchers evaluated the biocompatibility of the NPs with BeWo cells and primary human placental pericytes (hPC-PL) using a standard two-dimensional culture. Cell viability was reduced with increasing concentration and duration of NP exposure. Consequently, a NP concentration of 25 µg.cm^{-2} was selected for the studies on chip. The researchers reported that up to 4% of negatively charged nanoparticles can pass the barrier, in a time-dependent manner. In another study, Yin et al.[40] used a PMPS model to evaluate the effect of titanium dioxide (TiO_2) NPs on pregnant women. The device was made with PDMS and presented three channels, one middle channel filled with the extracellular matrix Matrigel and two peripheral channels for the culture of HUVECs and BeWo cells, respectively. The peripheral channels were connected by microchannels to the central channel. The maternal microchannel was perfused with TiO_2 NPs at a concentration of 50 or 200 µg/mL, with a flow rate of 20 µL/h for 24 h, followed by a perfusion of THP-1 cells for 30 minutes at a flow rate of 40 µL/h. At low concentrations of NPs, the authors reported impaired immune cell behavior and dysfunctions of placental barrier despite no significant change in the dead cells ratio nor in the production of reactive oxygen species (ROS). With high concentrations of NPs the dead cell increased correlated to the increase of ROS. In another study, Schuller et al.[41] evaluated the effects of NP exposure on the human placental barrier by developing a PMPS platform with integrated impedance microsensor arrays. The sensors were connected to a porous PET membrane and BeWo cells were seeded on the apical side of the membrane. The cells were then exposed to TiO_2, silicon dioxide (SiO_2), and three different concentrations of zinc oxide (ZnO) NPs. The integrity of the barrier remained after exposure to TiO_2 and SiO_2 NPs, but it was reduced after treatment with ZnO NPs already after 4 h of exposure. ZnO also led to an increase in ROS production directly proportional to the concentration of NPs and time after exposure. One type of nanoparticle that has caught the attention of researchers in the field of drug delivery is the nanoliposome, since it is very effective and biocompatible. Subsequently, Abostait et al.[42] explored the impact of NPs exposure on trophoblast syncytialization and microvilli formation using a dynamic PMPS model. BeWo cells were cultured in the device (dynamic condition) and in 24-well plates (static condition) and were subjected or not (control) to forskolin for 48 h. The cells were then perfused with chondroitin sulfate-conjugated liposomes at a concentration of 1.25 × 10^9 particles/mL at 37 °C, 5% CO_2 for 8 h and the uptake of liposome by the cells was evaluated. Greater microvilli formation and syncytialization were registered in the dynamic cell culture condition compared to static conditions. Moreover, liposome uptake by cells was also greater in dynamic conditions and with greater forskolin time exposure.

Table 3. Placental MPS models and cell lines used in recent studies of toxicology screening. The figures are reprinted with permission from Zhu et al. [29] Copyright (2018) American Chemical Society; Cao et al. [33] Copyright (2023) The Authors (open access); Blundell et al. [36] Copyright (2017) Wiley VCH Verlag GmbH & Co; Pemathilaka et al. [37] Copyright (2019) The Authors (open access); Yin et al. [40] Copyright (2018) Elsevier Ltd; Abostait et al. [42] Copyright (2022) American Chemical Society; Schuller et al. [41] Copyright (2020) Elsevier B. V.; and adapted with permission from Blundell et al., 2016 [30] Copyright (2016) the Royal Society of Chemistry; Lee et al., 2015 [31] Copyright (2015) Taylor & Francis; Pu et al. 2021 [32] Copyright (2021) the Royal Society of Chemistry; and Richardson et al. [34] Copyright (2022) the Royal Society of Chemistry (open access).

Placenta-on-Chip	General Description	Cell Lines	Ref.
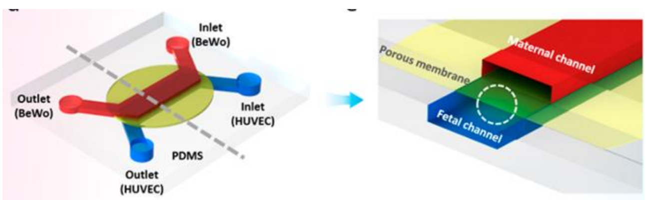	Diagram of the multilayered chip's design and construction in vitro to mirror the human placental barrier. The top layer is the maternal channel, the middle layer is a porous membrane, and the bottom layer is the fetal channel. The microdevice was built of PDMS, which is biocompatible. A placental barrier was built with HUVEC and BeWo epithelial layers on either side of the membrane. The flow approximated the dynamic setting of an in vivo placenta. HUVECs: human umbilical vein endothelial cells PDMS: Polydimethylsiloxane	BeWo, HUVEC	29

<table>
<tr><th>Placenta-on-Chip</th><th>General Description</th><th>Cell Lines</th><th>Ref.</th></tr>
<tr><td>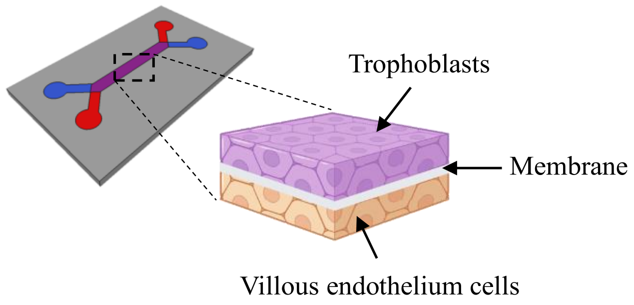
</td><td>An illustration of the microengineered technology that recreates the three-dimensional microarchitecture of the placental barrier. A thin, semipermeable membrane divides the upper and bottom microchannels of the PMPS. On the apical side of the membrane, the top microchannel is used to cultivate trophoblast cells, and the lower microchannel is used to cultivate villous endothelium cells.</td><td>HPVECs,
BeWo</td><td>30</td></tr>
<tr><td>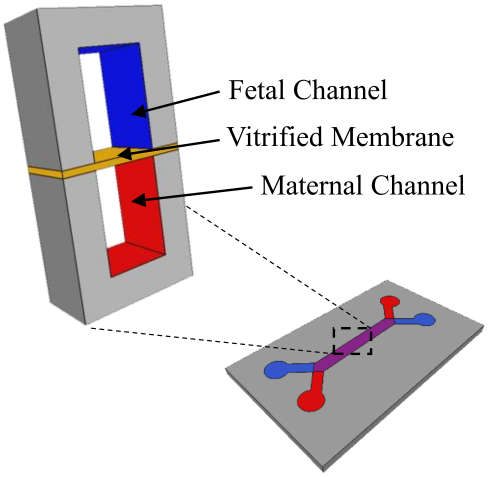
</td><td>PMPS technology: The upper (blue) and bottom (red) PDMS chambers of the microengineered device are connected by a vitrified collagen membrane. In the placenta-on-a-chip technology, endothelial and trophoblast cells are co-cultured in close apposition on the opposing sides of the intervening membrane to generate a microengineered placental barrier.</td><td>JEG-3 cells,
HUVECs</td><td>31</td></tr>
<tr><td></td><td>Schematic of a 3D microfluidic chip made of PDMS showing the following parts: Two outer channels (blue), each supplied by a linear channel with an inlet and outlet, and a third pillar barrier in between. One central compartment (red) supplied by a central linear channel with two inlet and two outlet ports.
CW: Outer channels width
BW: Pillar barrier width
PS: Pillar spacing</td><td>HTR8/SVneo
HUVECs</td><td>32</td></tr>
<tr><td>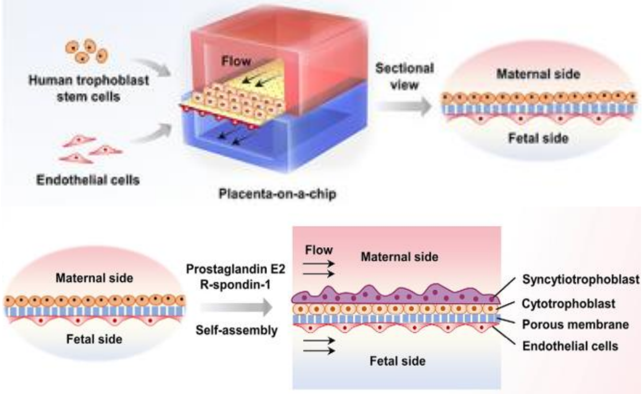
</td><td>Model of the biomimetic placental barrier shown schematically. On the upper channel, hTSCs were seeded to create the bilayered trophoblastic epithelium. To replicate the fetal endothelium, HUVECs were grown on the opposite side of a collagen-coated membrane.
hTSCs: Human Trophoblast Stem Cells
HUVECs: human umbilical vein endothelial cells</td><td>hTSCs,
HUVECs</td><td>33</td></tr>
</table>

Placenta-on-Chip	General Description	Cell Lines	Ref.
FMi-OOC 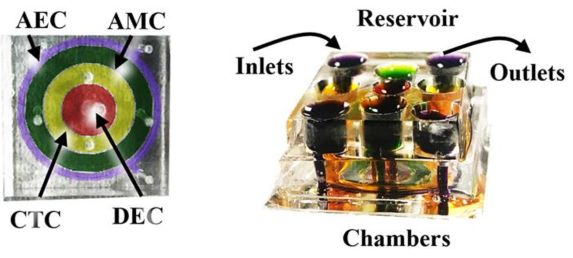 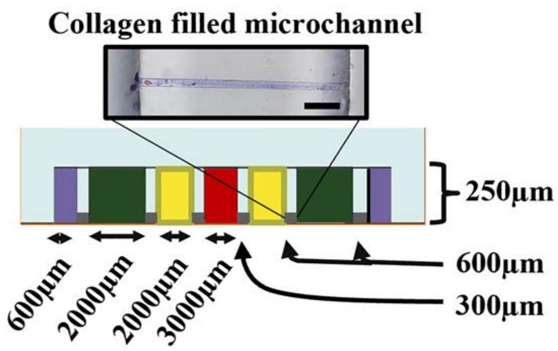 PLA-OOC 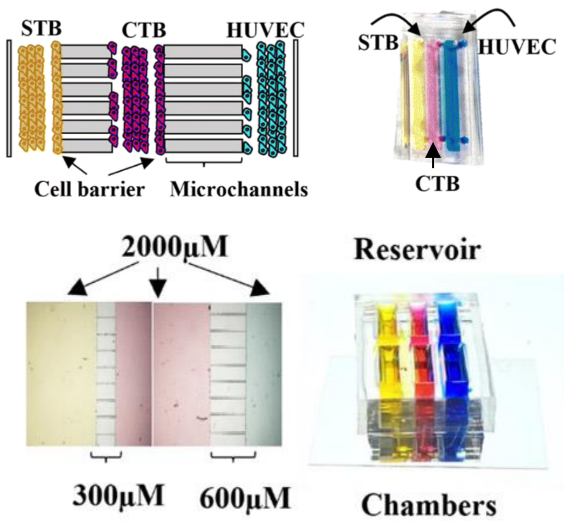	FMi-OOC device used to model the fetal membrane amniochorion-decidua interface. DEC (red), CTCs (yellow), AMCs (green), and AECs (purple) were seeded, from the center to the periphery, respectively. Microchannels connecting culture chambers were filled with collagen (visible through staining with Masson trichome). Scale bar:100 µm FMi-OOC: Feto-maternal interface Organ-on-chip DEC: Decidua cell CTC: Chorion trophoblast cell AMC: Amniotic mesenchymal cell AEC: Amniotic epithelial cell PLA-OOC device used to model the trophoblast–endothelial interface. Syncytialized BeWo cells producing the STB layer (yellow), BeWo cells reconstructing the CTB layer (pink), and HUVECs forming the endothelium layer (blue) were seeded, from left to right, respectively, on the device. The reservoirs of the chip allowed for 24h perfusion. PLA-OOC: Placenta Organ-on-Chip STB: Syncytiotrophoblast CTB: Cytotrophoblast HUVECs: Human umbilical vein endothelial cells	DEC, CTC, AMC, AEC BeWo, HUVEC	34
	FMi-OOC device used to model the fetal membrane amniochorion-decidua interface. DEC (red), CTCs (yellow), AMCs (green), and AECs (purple) were seeded, from the center to the periphery, respectively. Microchannels connecting culture chambers were filled with collagen (visible through staining with Masson trichome). Scale bar:100 µm FMi: Feto-maternal interface DEC: Decidua cell CTC: Chorion trophoblast cell AMC: Amniotic mesenchymal cell AEC: Amniotic epithelial cell	DEC, CTC, AMC, AEC	35

Placenta-on-Chip	General Description	Cell Lines	Ref.
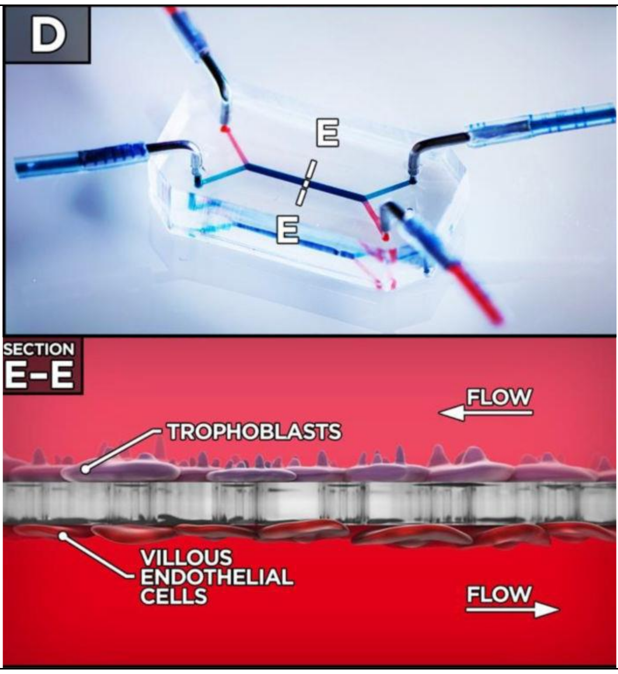	Isometric and cross-section view of the microengineered replica of the placental barrier's multi-layered, three-dimensional architecture. The model included a trophoblast and endothelial cells co-culture on either side of a thin porous polymeric membrane inside the device. The viability of the cells was preserved during culture by maintaining a constant layer of culture media on both sides of the membrane.	BeWo, HPVECs	36
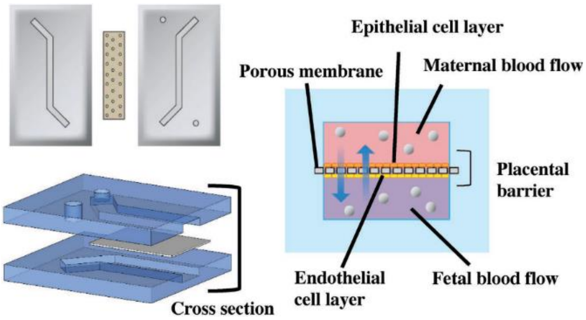	Schematic of the top and bottom layers of the device separated by a porous membrane. The top channel corresponds to the maternal side and the bottom to the fetal side.	BeWo, HUVEC	37
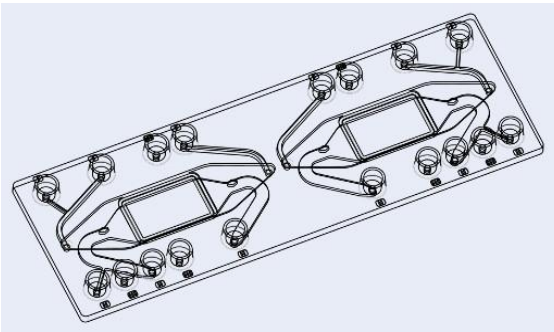	Schematic of the chip Fluidic 653 from Microfluidic ChipShop used for the experiments. BeWo cells were added to the apical channel (upper side) of the biochip on day 0 and hPC-PL cells were added to the basolateral channel (lower side) on day 1. From day 3, a peristaltic pump was connected to the apical channel of the biochip, providing a closed circulation of medium at a continuous flowrate of 44 µL min−1. Following four days of fluidic incubation, the reservoir's medium was replaced by a medium-nanoparticle solution.	BeWo, hPC–PL	38
	Real and schematic pictographs of the microdevice with a 3D placental barrier model. Two parallel cell microchannels and one center matrix microchannel are presented in the model. TiO_2-NPs were added to the maternal side of the device to simulate environmental exposure to nanoparticles.	BeWo, HUVEC	40

Placenta-on-Chip	General Description	Cell Lines	Ref.
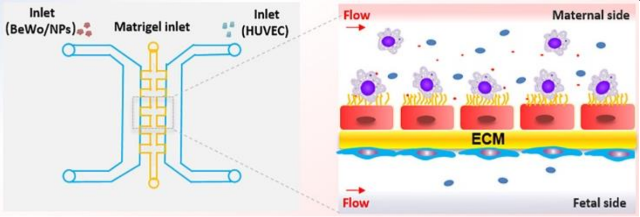	HUVEC: human umbilical vein endothelial cells TiO_2: Titanium Dioxide NPs: Nanoparticles		
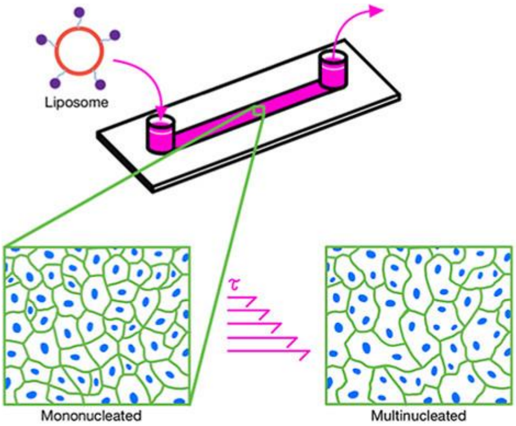	Schematic of the designed dynamic placenta-on-a-chip model to test chemical uptake and dynamic flow effects. BeWo cells presented different degrees of syncytialization through chemical induction.	BeWo	42
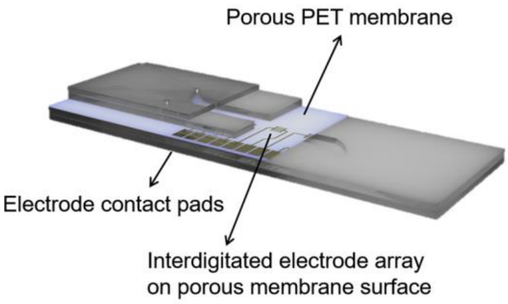	Schematic of the highly integrated MPS for assessing nanomaterial risk at the placental barrier. The model includes an IDES impedance biosensor array manufactured on the PET membrane between the mother and fetal channels. MPS: Microphysiological Systems IDES: Interdigitated Electrode Structures PET: Polyethylene terephthalate	BeWo	41

PMPS devices have been proving to be valuable resources for the study of several aspects of human pregnancy. A representation of the PMPS devices and respective cell lines used on the studies above is presented in Table 1, 2 and 3. Several reports showed that the results obtained in such devices are in greater conformity with what is observed *in vivo* than those obtained in well-plate assays. However, some limitations still need to be overcome. For instance, several studies still use cancer-derived cells, and how accurately these cells depict the normal epithelium present in the placenta is questionable[30]. Also, some culture conditions need to be optimized through the control of fluid flow rate and shear stress in the culture chambers[31].

Other placenta related models

The establishment of cell cultures that recapitulate the physiological factors found *in vivo* is critical to achieve accurate results *in vitro* and to reproduce what is observed in the human body. Haider et al.[43] used purified first-trimester cytotrophoblasts to establish long-term expanding cytotrophoblast organoid cultures. The organoids showed stemness and proliferative properties and could grow and differentiate under defined culture conditions. For instance, the removal of self-renewal-promoting factors caused trophoblasts to develop and express NOTCH1, which led to the emergence of nearby EVTs. Recently, Hori et al.[44] developed an organoid and a column barrier model to replicate the chorionic villus found in the placenta. This structure presents an outer layer of syncytiotrophoblast cells STs and an inner layer of cytotrophoblast cells (CTs). The organoids were formed in micro-scale size agarose wells using TSs. These cells have a similar function than CTs and can be handled for longer periods of time. After a 3-step treatment with different culture media, the authors obtained organoids with an outer layer of STs with the TSs inside that remained undifferentiated. The presence of microvilli on the ST cell layer was also reported, similar to what is observed *in vivo*. For a more accurate study of permeability, the authors developed column-type barrier models with TSs on the apical side and HUVECs on the basal side. TS differentiation into ST was also induced with a 3-step treatment using different media. The apparent permeability coefficient for caffeine, antipyrine and glyphosate was evaluated with the ST barrier model. The authors reported a similar tendency from what was verified in *ex vivo* studies: low coefficient for glyphosate and higher coefficients for caffeine and antipyrine. However, the difference between those coefficients was not as pronounced as in other studies. In another study, Li et al.[45] recently established an organoid system to study the role of uNKs in EVT invasion to the uterine mucosa. They found that four cytokines (XCL1, CSF2, CSF1, and CCL5) produced by uNKs acted on EVTs through specific receptors and regulated their behavior. These cytokines not only help in differentiation and invasion of EVTs but play an important role in increasing the blood flow and nutrients for the optimal growth of the fetus. Results from ELISA showed enhanced EVT invasion using a co-culture for metalloproteinase proteins.

Three-dimensional (3D) printing is also a potential resource for the improvement of placenta models. Kuo et al.[46] bioengineered a placenta model through shear wave elastography and 3D bioprinting to study possible preeclampsia treatments. Using a base of gelatin methacrylate (GelMA), BeWo cells and human mesenchymal stem cells (hMSCs) were loaded in the periphery of a spiral channel while EGF was printed on the center of the spiral. Cell migration towards the center was dose-dependent of EGF concentration with higher concentrations of EGF promoting a greater degree of trophoblast and hMSC migration. Consequently, EGF showed a potential to be used in the treatment of preeclampsia. In another study, Kuo et al.[47] developed a new placenta model for preeclampsia studies in which an endothelialized lumen and trophoblasts were bioprinted in a perfusion bioreactor. The bioreactor contributed to the increase of the expression of angiogenic markers and network formation by the endothelial cells through a positive correlation with shear stress. The trophoblasts, in turn, induced the apoptosis of endothelial cells whilst reducing angiogenic responses by diminishing endothelial motility rates and network formation. It was also reported that the trophoblast invasion rate was inhibited by the presence of endothelial cells. Furthermore, Ding et al.[48] designed 2D and 3D models to study the trophoblast invasion. The models consisted of multi-rings or multi-stripes made by bioprinting GelMA with HTR-8/SVneo trophoblasts. Using these models, the researchers evaluated the effects of different gradients of the chemoattractant EGF on the trophoblasts. In 2D models the invasion was faster than in 3D models due to the effects of cell proliferation and migration. The inclusion of a cell-free GelMA layer to the 3D models reduced these effects so that the presence of EGF was the most influential factor. The invasion rates were 13 ± 5 µm/day and 21 ± 3 µm/day on the multi-ring and on the multi-strip model, respectively. Without the presence of EGF, the invasion rate was 5 ± 4 µm/day. The multi-strip model can be further improved by adding more strips with other relevant structural or analytical components.

Finding the ideal co-culture conditions that allows the formation of continuous cell layers over the desired surfaces is still a challenge that researchers are addressing in current studies.

The reported placenta related models are summarized in Table 4.

Table 4. Placental MPS models in recent studies that were used to evaluate villi formation using mono-cell culture or organoids, and that used bioprinting. The figures are reprinted with permission from Haider et al. [43] Copyright (2018) The Author(s) (open access); Hori et al. [44] Copyright (2024) The Author(s) (open access); Li et al. [45] Copyright (2023) The Author(s) (open access); Kuo et al. [46] Copyright (2016) American Chemical Society; Kuo et al. [47] Copyright (2018) Wiley Periodicals, Inc.; and Ding et al. [48] Copyright (2019) The Author(s) (open access).

Placenta Model	General Description	Cell Lines	Ref.
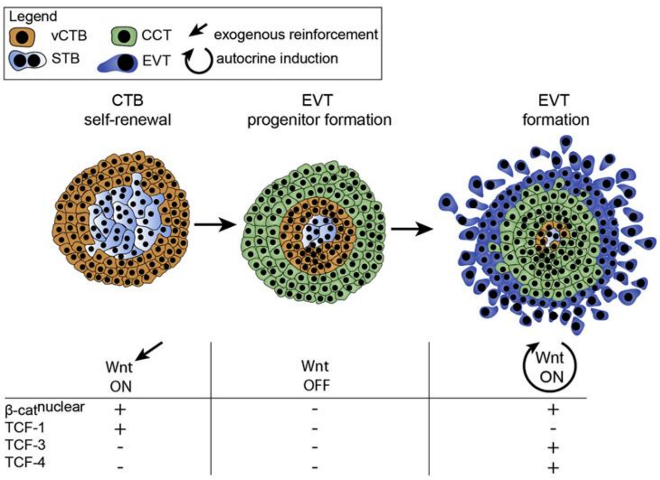	Schematic model demonstrating the function of Wnt in the self-renewal and differentiation of trophoblast organoids. TCF: T cell factor β-cat: β-catenin CTB: cytotrophoblast EVT: extravillous trophoblast STB: syncytiotrophoblast	Villous CTBs	43
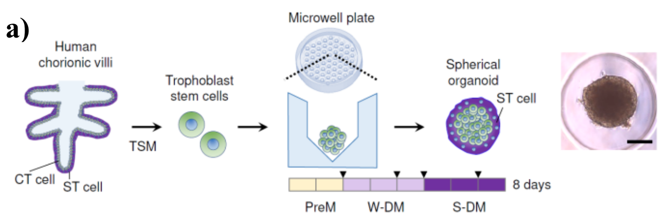	Chorionic villi models. a) Organoid model formed in microwells. b) Column-type ST barrier model PreM: Pre-culture medium W-DM: Weak differentiation medium S-DM: Strong differentiation medium	SDC1-GFP TS cells HUVEC	44

Placenta Model	General Description	Cell Lines	Ref.
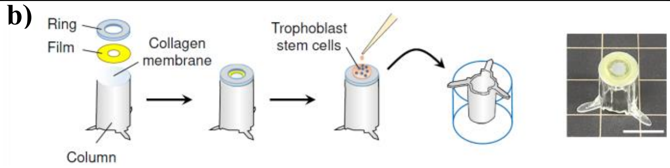			
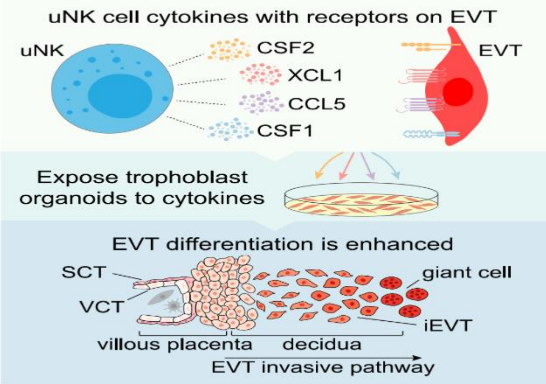	Cytokines such as XCL1, CSF2, CSF1, and CCL5 are produced by uNK and enhanced EVT invasion	uNK	45
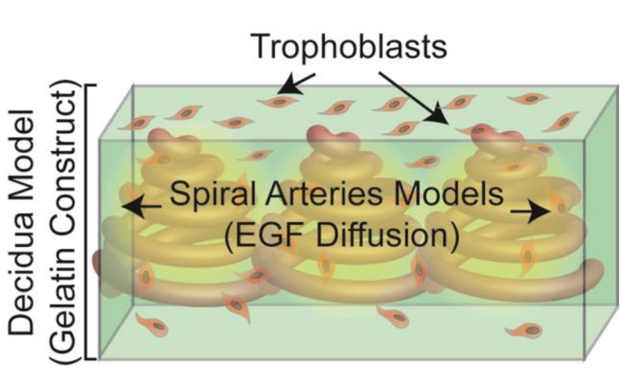	Schematic of the bioengineered placenta model. The model is built on a cylindrical GelMA hydrogel previously loaded with various components at various radial points. The model's edge is printed with a trophoblastic shell enclosed within it. A radial concentration gradient is created by the chemoattractant EGF, which is printed in the construct's core and diffuses outward. Trophoblasts move toward the center along the concentration gradient.	BeWo, hMSCs	46
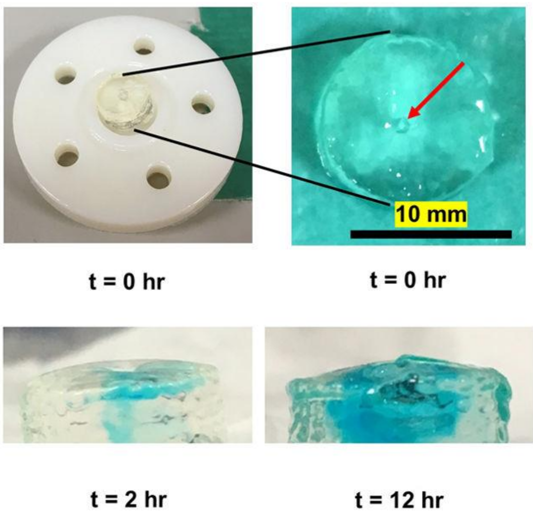	Dynamic bioprinted placenta model with a 3D printed perfusion bioreactor system. The placenta model's position in relation to the 3D-printed reactor chamber was shown in the top left image, which was enlarged in the image on the right. The bioprinted placenta model featured a patent channel in the center (red arrow) and was cylindrical in shape (diameter: 10 mm; height: 2 mm). After 12 hours of perfusion, a blue dye was used to show that material diffused radially outward from the core lumen, demonstrating the existence of interstitial flow.	HUVEC HTR8	47

Placenta Model	General Description	Cell Lines	Ref.
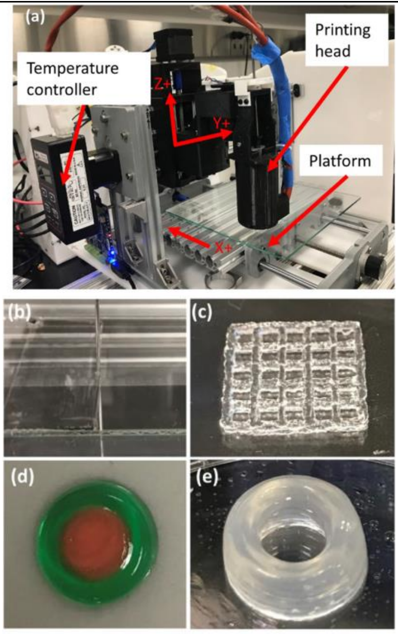	a) The setup of the bioprinting system. (b-e) A variety of bioprinted 3D constructions, including tubular, lattice, double ring, and single layer sheets.	HTR-8	48

Endometrium Microphysiological Systems

The endometrium is a tissue of the uterus that has a crucial role in the establishment of a healthy pregnancy. Ostrovidov et al.[49] was among the firsts to use a microfluidic device for coculturing mouse endometrial cells and mouse embryos under perfusion. The device integrated a chamber separated in two parts by a polyester membrane use as a substrate for endometrial cell culture. The device was perfused from the bottom chamber and the embryos were culture on the endometrial cells in the top chamber. The results showed that the development of embryos to morulae-blastocysts in perfused microfluidic device was significantly faster than in microdrop culture[49]. An optimized version of the device was made and donated human embryos were cultured for 72 h in the microfluidic chamber with human donated endometrial cells (EMCs). The device was perfused from the bottom chamber. The developed blastocyst quality was evaluated by Gardner's score. The results showed enhance number of embryos reaching the blastocyst stage in microfluidic device 73.7% (14/19) compared to microdrop culture 45% (9/20). Moreover, the quality of the blastocysts over 3AB Gardner score was improved in the device 42.9% (6/14) compared to 22.2% (2/9) in microdrop culture. The cell number in the blastocysts was also higher for blastocysts in the microfluidic device[50]. More recently, De Bem et al.[51] investigated the impact of glucose and insulin levels on epithelial and stromal endometrial cells. The cells were isolated from nonpregnant cows and seeded respectively on the upper and lower chambers of a microfluidic device separated by a porous membrane. Insulin concentrations at 1 and 10 ng/mL and glucose at 0.5, 5, and 50 mM were perfused for 72 hours at a flow rate of 1 µL/minute. The authors reported that variations in insulin affected the quantitative secretion of 196 proteins whilst high glucose values modified 21 and 191 protein-coding genes and the secretion of 1 and 23 proteins in epithelial and stromal cells, respectively. Consequently, this model showed that metabolic factors can influence the endometrial function, playing an important role in achieving a pregnancy. Moreover, Ahn et al.[52] developed a microfluidic device that replicates the endometrial microenvironment and evaluated the effect of levonorgestrel on the cell culture. The device was composed of five microchannels, two central channels for the culture of stromal fibroblasts and endothelial cells, an outermost channel for endometrial stromal fibroblasts and the remaining channels for culture medium perfusion. To simulate different phases of the menstrual cycle, the cell cultures were treated with different levels of progesterone and oestradiol. Exogenous pro-angiogenic factors were also added to some of them. Following drug treatment, blood vessel regression and increased endometrial permeability were observed in a dose-dependent manner. Therefore, this platform is relevant for the understanding of the cellular mechanisms behind the female reproductive cycle and pregnancy.

A summary of the above reported endometrium microphysiological systems is presented in Table 5.

Table 5. Endometrium MPS models and cell lines used in recent studies. The figures are reprinted with permission from Ostrovidov et al. [49] Copyright (2005) Transducer Research Fundation; Mizuno et al. [50] Copyright (2007) American Society for Reproductive Medicine. Published

Endometrium Model	General Description	Cell Lines	Ref.
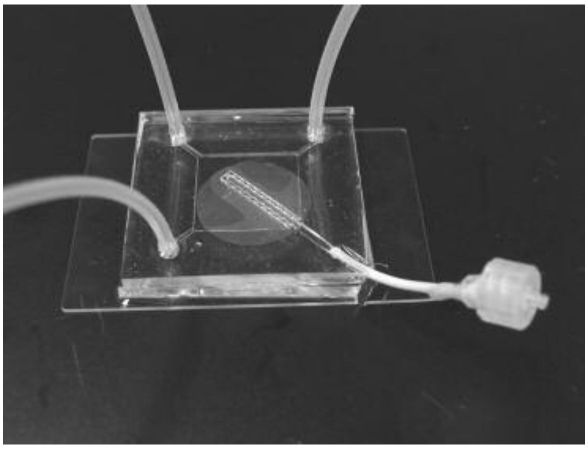	Photo of a microfluidic device for assisted reproductive technology (ART), which includes a chamber separated in two parts by a permeable membrane. Endometrial cells were cultured on the membrane. The device was perfused in the bottom chamber while the embryos were cultured on the endometrial cells in the top chamber.	Mouse endometrial cells and mouse embryos	49
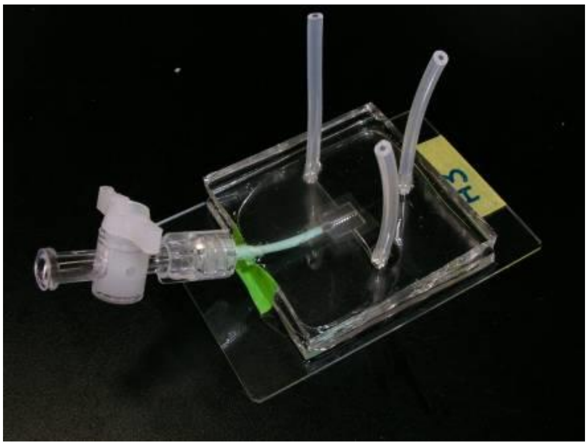	Previous microfluidic device for ART optimized. A polyester guide with a valve were included to allow easy loading and harvesting of the human embryos via long pipette tip. The device was perfused in the bottom chamber while the human embryos were cultured in a cage on the donated human endometrial cells in the top chamber.	Donated human endometrial cells and donated human embryos	50
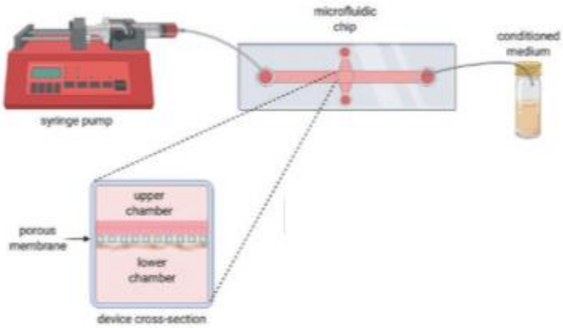	Schematic illustration of the experimental design and endometrium MPS device used to replicate the physiological extremes of glucose and insulin. For both trials, the flow rate was carried out at 1 µL/min every 72 hours.	Bovine endometrial cells	51

<table>
<tr><th>Endometrium Model</th><th>General Description</th><th>Cell Lines</th><th>Ref.</th></tr>
<tr><td>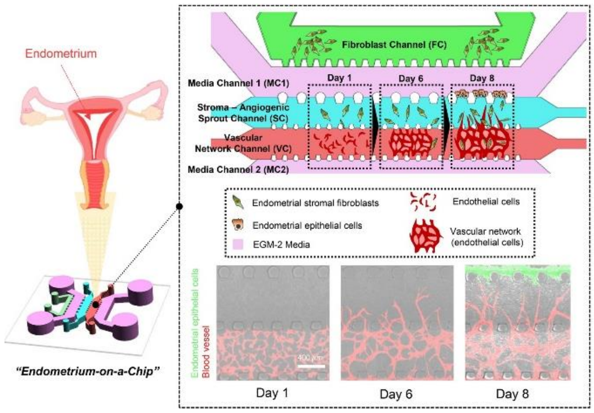
</td><td>Schematic of the 3D vascularized endometrial microenvironment reconstruction with an MPS. On day 1 the channel SC was loaded with CRL-4003-embedded fibrin gel solution, while the channel VC was loaded with EC-embedded fibrin gel. The outermost channel was loaded with extra endometrial stromal fibroblasts, to stimulate ECs to become pro-angiogenic by secreting biochemical signals. Both media channels were filled with EGM-2 culture medium. On day 8, EECs were infused into the media channel closer to SC.</td><td>HUVECs, Ishikawa cells, CRL-4003 cells</td><td>52</td></tr>
</table>

Conclusions

The study of human pregnancy is continually advancing through the efforts of researchers in developing in vitro models that overcome the limitations of animal models and standard 2D cell culture models.

Recent studies have been successful in recreating some of the phenomena that is observed in vivo, such as migration and implantation of trophoblast cells, microvilli formation, remodeling of arteries, and the presence of specific chemicals and proteins. These models contributed to the study of implantation, preeclampsia, and drug and nanoparticle transport and permeability through the placenta.

Despite the success in recreating cellular behaviors and in evaluating the effects of specific chemical factors, drugs, and nanoparticles, these models are yet to be refined. For instance, a great majority of the devices are made of PDMS, which, due to its hydrophobicity, is able to adsorb small hydrophobic molecules. Other devices incorporate hydrogels to better recreate the ECM environment. However, the ideal physical and chemical parameters for these hydrogels remain to be harnessed and optimized. Another matter to be improved is the development of models with the capacity to allow testing of many drugs at once or even having a perfusion system able to recreate the dynamic flow conditions found in vivo. Additionally, the majority of studies are limited to using only two cell types; some of them do not involve trophoblast cell line differentiation into syncytium nor the incorporation of certain pathology-related cell types such as decidual natural killer cells, macrophages, and inflammatory cells. It should also be acknowledged that the current models are still simple approximations of the great complexity of the human system. The improvements of PMPS devices and other MPS will contribute to the establishment of a systematic and cost-effective model allowing to effectively understand the mechanisms of human gestation, as well as the pathologies that occur, and inform and introduce prospects for their respective treatment.

Conflicts of interest

T.H. and H.K. own stock as members of a company, HPS Inc., and they potentially would receive compensation from the company. The remaining authors declare no competing interests.

Data availability

No primary research results, software or code have been included and no new data were generated or analysed as part of this review.

Acknowledgements

I. M. Gonçalves acknowledges FCT for the grant SFRH/BD/08646/2020. The authors are also grateful to FCT for partially financing the research through project PTDC/EMETED/7801/2020 and UIPD/50009/2020-FCT and UIDB/50009 – FCT. A.S. Moita also acknowledges FCT for partially financing her contract through CEECINST/00043/2021/CP2797/CT0005, doi: 10.54499/CEECINST/00043/2021/CP2797/CT0005. The authors acknowledge the financial support (4004) from the RCBE from Tokyo Medical and Dental University, Japan. The authors also acknowledge the partial financial support of the projects, PTDC/EEI-EEE/2846/2021 (https://doi.org/10.54499/PTDC/EEI-EEE/2846/2021) and 2022.06207.PTDC (https://doi.org/10.54499/2022.06207.PTDC) through national funds (OE), within the scope of the Scientific Research and Technological Development Projects (IC&DT) program in all scientific domains (PTDC), through the Foundation for Science and Technology, I.P. (FCT, I.P). The authors also acknowledge the partial financial support within the R&D Units Project Scope: UIDB/04077/2020, UIDB/00532/2020 and LA/P/0045/2020 (ALiCE). The authors also acknowledge the partial financial support by JSPS KAKENHI (Grant Numbers 23H01821, 22K18936 and 21K04852) (T.H. and H.K.), the Mandom International

Research Grants on Alternatives to Animal Experiments (T.H.), AMED-CREST (Grant Number JP21gm1310001) (H.K.), the JST Adaptable and Seamless Technology Transfer Program through Target-driven R&D (Grant Numbers JPMJTM22BD) (H.K.), the Research Center for Biomedical Engineering (T.H. and H.K.), and TMDU priority research areas grant (T.H.).

References

1 C. Gundacker and I. Ellinger, *Reprod. Toxicol.*, 2020, **96**, 273–281.
2 S. Shibata, E. H. Kobayashi, N. Kobayashi, A. Oike, H. Okae and T. Arima, *Reprod. Med. Biol.*, 2020, **19**, 301–313.
3 R. Tutar and B. Çelebi-Saltik, *Cells Tissues Organs*, 2022, **06100**, 36–45.
4 M. Cherubini, S. Erickson and K. Haase, *Micromachines*, 2021, **12**, 884.
5 S. Yang, Z. Chen, Y. Cheng, T. Liu, Lihong Yin, Y. Pu and G. Liang, *Environ. Pollut.*, 2021, **268**, 115861.
6 D. Bačenková, M. Trebuňová, D. Čížková, R. Hudák, E. Dosedla, A. Findrik-Balogová and J. Živčák, *Biomedicines*, 2022, **10**, 904.
7 H. Okae, H. Toh, T. Sato, H. Hiura, S. Takahashi, K. Shirane, Y. Kabayama, M. Suyama, H. Sasaki and T. Arima, *Cell Stem Cell*, 2018, **22**, 50-63.e6.
8 H. M. Dusza, J. van Boxel, M. B. M. van Duursen, M. M. Forsberg, J. Legler and K. H. Vähäkangas, *Sci. Total Environ.*, 2023, **860**, 160403.
9 R. O. Rodrigues, P. C. Sousa, J. Gaspar, M. Bañobre-López, R. Lima and G. Minas, *Small*, 2020, **16**, 2003517.
10 Q. Wu, J. Liu, X. Wang, L. Feng, J. Wu, X. Zhu, W. Wen and X. Gong, *Biomed. Eng. Online*, 2020, **19**, 9.
11 V. Faustino, S. O. Catarino, R. Lima and G. Minas, *J. Biomech.*, 2016, **49**, 2280–2292.
12 S. O. Catarino, R. O. Rodrigues, D. Pinho, J. M. Miranda, G. Minas and R. Lima, *Micromachines*, 2019, **10**, 593.
13 R. Rodrigues, R. Lima, H. Gomes and A. Silva, *U.Porto J. Eng.*, 2017, **1**, 67–79.
14 V. Carvalho, I. Gonçalves, T. Lage, R. O. Rodrigues, G. Minas, S. F. C. F. Teixeira, A. S. Moita, T. Hori, H. Kaji and R. A. Lima, *Sensors*, 2021, **21**, 3304.
15 Q. Yang, Q. Lian and F. Xu, *Biomicrofluidics*, 2017, **11**, 31301.
16 A. M. Ghaemmaghami, M. J. Hancock, H. Harrington, H. Kaji and A. Khademhosseini, *Drug Discov. Today*, 2012, **17**, 173–181.
17 I. M. Gonçalves, R. O. Rodrigues, A. S. Moita, T. Hori, H. Kaji, R. A. Lima and G. Minas, *Bioprinting*, 2022, **26**, e00202.
18 I. Miranda, A. Souza, P. Sousa, J. Ribeiro, E. M. S. Castanheira, R. Lima and G. Minas, *J. Funct. Biomater.*, 2021, **13**, 2.
19 C. M. Leung, P. de Haan, K. Ronaldson-Bouchard, G.-A. Kim, J. Ko, H. S. Rho, Z. Chen, P. Habibovic, N. L. Jeon, S. Takayama, M. L. Shuler, G. Vunjak-Novakovic, O. Frey, E. Verpoorte and Y.-C. Toh, *Nat. Rev. Methods Prim.*, 2022, **2**, 33.
20 E. Sano, C. Mori, N. Matsuoka, Y. Ozaki, K. Yagi, A. Wada, K. Tashima, S. Yamasaki, K. Tanabe, K. Yano and Y. Torisawa, *Micromachines*, 2019, **10**, 793.
21 N. Govindasamy, H. Long, H. W. Jeong, R. Raman, B. Özcifci, S. Probst, S. J. Arnold, K. Riehemann, A. Ranga, R. H. Adams, B. Trappmann and I. Bedzhov, *Dev. Cell*, 2021, **56**, 3276-3287.e8.
22 S. Miura, K. Sato, M. Kato-Negishi, T. Teshima and S. Takeuchi, *Nat. Commun.*, 2015, **6**, 8871.
23 J. Y. Park, S. Mani, G. Clair, H. M. Olson, V. L. Paurus, C. K. Ansong, C. Blundell, R. Young, J. Kanter, S. Gordon, A. Y. Yi, M. Mainigi and D. D. Huh, *Nat. Commun.*, 2022, **13**, 1252.
24 Y. Abbas, C. M. Oefner, W. J. Polacheck, L. Gardner, L. Farrell, A. Sharkey, R. Kamm, A. Moffett and M. L. Oyen, *J. R. Soc. Interface*, 2017, **14**, 20170131.
25 B. Mosavati, A. V Oleinikov and E. Du, *Int. J. Mol. Sci.*, 2020, **21**, 8755.
26 G. Rabussier, I. Bünter, J. Bouwhuis, C. Soragni, C. P. Ng, K. Dormansky, L. J. de Windt, P. Vulto, C. E. Murdoch, K. M. Bircsak and H. L. Lanz, *bioRxiv*, 2022, 2022.06.30.498115.
27 G. Rabussier, I. Bünter, J. Bouwhuis, C. Soragni, T. van Zijp, C. P. Ng, K. Domansky, L. J. de Windt, P. Vulto, C. E. Murdoch, K. M. Bircsak and H. L. Lanz, *Acta Biomater.*, 2023, **164**, 363–376.
28 S. M. Ghorbanpour, C. Richards, D. Pienaar, K. Sesperez, H. Aboulkheyr Es, V. N. Nikolic, N. Karadzov Orlic, Z. Mikovic, M. Stefanovic, Z. Cakic, A. Alqudah, L. Cole, C. Gorrie, K. McGrath, M. M. Kavurma, M. Ebrahimi Warkiani and L. McClements, *Cell. Mol. Life Sci.*, 2023, **80**, 1–27.
29 Y. Zhu, F. Yin, H. Wang, L. Wang, J. Yuan and J. Qin, *ACS Biomater. Sci. Eng.*, 2018, **4**, 3356–3363.
30 C. Blundell, E. R. Tess, A. S. R. Schanzer, C. Coutifaris, E. J. Su, S. Parry and D. Huh, *Lab Chip*, 2016, **16**, 3065–3073.
31 J. S. Lee, R. Romero, Y. M. Han, H. C. Kim, C. J. Kim, J.-S. Hong and D. Huh, *J. Matern. Neonatal Med.*, 2016, **29**, 1046–1054.
32 Y. Pu, J. Gingrich and A. Veiga-Lopez, *Lab Chip*, 2021, **21**, 546–557.
33 R. Cao, Y. Wang, J. Liu, L. Rong and J. Qin, *Cell Prolif.*, , DOI:10.1111/cpr.13469.
34 L. S. Richardson, A. K. Kammala, M. M. Costantine, S. J. Fortunato, E. Radnaa, S. Kim, R. N. Taylor, A. Han and R. Menon, *Lab Chip*, 2022, **38**, 4574–4592.
35 S. Kim, L. Richardson, E. Radnaa, Z. Chen, I. Rusyn, R. Menon and A. Han, *J. Hazard. Mater.*, 2022, **422**, 126759.
36 C. Blundell, Y. Yi, L. Ma, E. R. Tess, M. J. Farrell, A. Georgescu, L. M. Aleksunes and D. Huh, *Adv. Healthc. Mater.*, 2018, **7**, 1700786.
37 R. L. Pemathilaka, J. D. Caplin, S. S. Aykar, R. Montazami and N. N. Hashemi, *Glob. Challenges*, 2019, **3**, 1800112.
38 L. J. Gresing, P. Radon, R. P. Friedrich, D. Zahn, M. Raasch, A. S. Mosig, S. Dutz, C. Alexiou, F. Wiekhorst, A. Hochhaus and J. H. Clement, *J. Magn. Magn. Mater.*, 2021, **521**, 167535.
39 Microfluidic ChipShop, Fluidic 653, https://www.microfluidic-chipshop.com/catalogue/microfluidic-chips/polymer-

chips/membrane-chips/membrane-chips-fluidic-653/.
40 F. Yin, Y. Zhu, M. Zhang, H. Yu, W. Chen and J. Qin, *Toxicol. Vitr.*, 2019, **54**, 105–113.
41 P. Schuller, M. Rothbauer, S. R. A. A. Kratz, G. Höll, P. Taus, M. Schinnerl, J. Genser, N. Bastus, O. H. Moriones, V. Puntes, B. Huppertz, M. Siwetz, H. Wanzenböck and P. Ertl, *Sensors Actuators, B Chem.*, 2020, **312**, 127946.
42 A. Abostait, J. Tyrrell, M. Abdelkarim, S. Shojaei, W. H. Tse, I. M. El-Sherbiny, R. Keijzer and H. I. Labouta, *Mol. Pharm.*, 2022, **19**, 3757–3769.
43 S. Haider, G. Meinhardt, L. Saleh, V. Kunihs, M. Gamperl, U. Kaindl, A. Ellinger, T. R. Burkard, C. Fiala, J. Pollheimer, S. Mendjan, P. A. Latos and M. Knöfler, *Stem Cell Reports*, 2018, **11**, 537–551.
44 T. Hori, H. Okae, S. Shibata, N. Kobayashi, E. H. Kobayashi, A. Oike, A. Sekiya, T. Arima and H. Kaji, *Nat. Commun.*, 2024, **15**, 962.
45 Q. Li, A. Sharkey, M. Sheridan, E. Magistrati, A. Arutyunyan, O. Huhn, C. Sancho-Serra, H. Anderson, N. McGovern, L. Esposito, R. Fernando, L. Gardner, R. Vento-Tormo, M. Y. Turco and A. Moffett, *Cell Stem Cell*, 2024, **31**, 181-195.e9.
46 C. Kuo, A. Eranki, J. K. Placone, K. R. Rhodes, H. Aranda-espinoza, R. Fernandes, J. P. Fisher and P. C. W. Kim, *ACS Biomater. Sci. Eng.*, 2016, **2**, 1817–1826.
47 C. Kuo, M. Shevchuk, J. Opfermann, T. Guo, J. P. Fisher and P. C. W. Kim, *Biotechnol. Bioeng.*, 2020, **116**, 181–192.
48 H. Ding, N. P. Illsley and R. C. Chang, *Sci. Rep.*, 2019, **9**, 18854.
49 S. Ostrovidov, J. Mizuno, H. Nakamura, H. Inui, Y. Sakai and T. Fujii, in *Proceedings of Micro Total Analysis Systems 2005 Conference*, 2005, pp. 361–363.
50 J. Mizuno, S. Ostrovidov, Y. Sakai, T. Fujii, H. Nakamura and H. Inui, *Fertil. Steril.*, 2007, **88**, S101.
51 T. H. C. De Bem, H. Tinning, E. J. R. Vasconcelos, D. Wang and N. Forde, *Endocrinol. (United States)*, 2021, **162**, 1–18.
52 J. Ahn, M. J. Yoon, S. H. Hong, H. Cha, D. Lee, H. S. Koo, J. E. Ko, J. Lee, S. Oh, N. L. Jeon and Y. J. Kang, *Hum. Reprod.*, 2021, **36**, 2720–2731.

Data availability

No primary research results, software or code have been included and no new data were generated or analysed as part of this review.